17th World Conference on Earthquake Engineering, 17WCEE
Sendai, Japan - September 13th to 18th 2020

DROP WEIGHT TEST OF POLYPROPYLENE FIBER REINFORCED CONCRETE WALL AFTER ONE-YEAR DRYING SHRINKAGE

Y. Sato[(1)], K. Naganuma[(2)] and Y. Kaneko[(3)]

[(1)] *Associate Professor, Kyoto University, Kyoto, Japan, sato.yuichi.7n@kyoto-u.ac.jp*
[(2)] *Professor, Nihon University, Tokyo, Japan, naganuma.kazuhiro@nihon-u.ac.jp*
[(3)] *Professor, Kyoto University, Kyoto, Japan, kaneko.yoshio.5e@kyoto-u.ac.jp*

Abstract

Recent progress of the finite element method for reinforced concrete (RC) enables to simulate the seismic vibration of whole structure of a building and indicates that drying shrinkage cracks affect the seismic resistant performances. Polypropylene fiber reinforced concrete (PFRC) is a promising material to reduce the vibration drift of building without modifying or adding the geometries of structural components since the fibers are expected to reduce the cracks and strains under the dying shrinkage. Wall is especially affected by the drying shrinkage among structural components of the RC. This paper attempts to observe and quantify the cracks and the vibration characteristics by means of drop-weight test and finite element analysis.

Four wall specimens of the same geometry and bar arrangement, named N0, NR, P0 and PR, are prepared. Geometry of the wall is 70 mm×700 mm×1050 mm and the reinforcement ratio 0.36%. The wall is connected with two columns on the sides. The column is 150 mm×150 mm in cross section and contains four longitudinal bars of 6 mm diameter and 0.25% hoops. Two kind of concrete materials (plain concrete for N0 and NR and PFRC for P0 and PR) are used. The compressive strength is around 45 N/mm^2 and the volume ratio of fiber 1.2%. For specimens NR and PR, the drying shrinkage deformations are restrained by fixing top and bottom of the wall part for a year. Each specimen is rotated 90° and fixed to a concrete block. A steel drop weight of 398.8 kg is hung by a magnet hanger and released from a height of 1.29 m. A constant velocity of 5 m/s is applied at the instance of collision. A load cell of 1000 kN capacity is inserted between the specimen and the drop weight. A displacement transducer are fixed to measure the drift. The sampling frequency is 5 kHz and the duration is 0.3 second. The recorded maximum drift varies from 0.637% to 0.678% and the maximum load from 717.2 kN to 780.1 kN, but influences of the fiber and the restraint are not observed. On the other hand, a large residual drift 0.150% is observed in the restrained specimen NR comparing to other three specimens. In addition, six cracks are observed in the mid parts of the wall and the columns of NR while only a crack is observed in each rest specimen. The test result indicates that the polypropylene fiber reduces the drying shrinkage cracks and residual deformation after the impact loading.

2D nonlinear finite element analyses are conducted to simulate the behaviors from drying shrinkage cracking up to the impact loading and to estimate the vibration characteristics. An orthotropic constitutive law is adopted for the concrete. This law consists of hysteresis path model that connects between compressive and tensile envelopes, shear transfer model across the cracked surface, and strain dependency models of compressive and tensile strengths. A model to discretize the crack distribution considering bond between the concrete and the reinforcing bars is adopted to trace the crack propagation under the shrinkage and the impact loading. The analysis results indicate that the polypropylene fiber prevents the elongation of natural period of the wall due to the drop-weight collision as well as the long period drying shrinkage.

Keywords: crack; impact loading; natural period; nonlinear finite element analysis; bond

1. Introduction

So far drying shrinkage cracking of reinforced concrete has been considered as problems of external aesthetics and one of causes of steel bar corrosion. However, several finite element analyses of full-modeled RC buildings, which are enabled by recent advancement in numerical techniques, indicate that the shrinkage cracking probably affects seismic performances of the structure [1, 2]. Conventional seismic resistant measurement such like increased cross section of columns and beams or additional stiffening members to reduce response drift may decrease usable floor area and aesthetical value. One of possible alternatives, which needs not to change the structural geometry, is fiber reinforced concrete. This study conducts low-velocity drop-weight tests of wall specimens made of polypropylene fiber reinforced concrete (PFRC) to quantitate how the PFRC reduce the damage and improve the vibration characteristics of the drying-shrinkage-sensitive RC wall. The behaviors of wall specimens are numerically reproduced by nonlinear finite element analyses to compare natural period changing during the vibration after the drop-weight collision between plain concrete and the PFRC.

2. Test

2.1 Specimens

Table 1 summarizes the specifications of the wall specimens and Fig. 1 shows the geometry. Experimental variables are fiber content in the concrete and the restraining of the shrinkage deformation. Four walls prepared in this study adopts the same geometry and bar arrangement to those of Specimen "NOP" in Iwamoto's experimental study [3] in the interest of the analytical investigation in the following section since the static behavior of NOP had been analyzed by a previous study [4]. The wall's geometry is 1050 × 700 × 70 mm with reinforcing plain bars of 4 mm with 50 mm spacing. The reinforcement ratio is 0.36%. The column cross section is 150 × 150 mm with four longitudinally deformed bars of 6 mm diameter (0.57%) and shear reinforcing plain bars of 4 mm diameter with 50 mm spacing (0.34%).

Specimens N0 and NR are made of a plain concrete while P0 and PR of the PFRC. Table 2 shows the mixture. This mixture is the same to that used in the authors' previous study [5]. An early strength Portland cement is used in an intension to increase the drying shrinkage strain. The plain concrete is made of the same mixture except the fiber. The fiber used in this study was polypropylene resin monofilament with an embossed surface. This type of fiber has length of 30 mm and equivalent diameter of 0.7 mm. The weight per a unit volume is 0.91 g/cm^3 and the maximum tensile strength is 500 N/mm^2. The fiber volume fraction is 1.2%.

Table 1 – Wall specimens

Specimen	Drying period (day)	Restraint	Concrete			Max. drift (%)	Residual drift (%)	Max. load (kN)
			Kind	Compressive strength (N/mm^2)	Shrinkage strain ($\times 10^{-3}$)			
N0	22	None	Plain	46.2	1.344	0.649	0.057	717.2
NR	372	Restrained	Plain	40.7	1.877	0.637	0.150	775.5
P0	21	None	PFRC	50.0	0.993	0.635	-0.015	780.1
PR	373	Restrained	PFRC	50.7	1.031	0.687	0.102	764.3

Table 2 –Mixture of polypropylene fiber reinforced concrete (per 1 m^3)

	Polypropylene fiber	W/C	Water	Cement	Sand	Gravel	Super plasticizer	Air
PP	10.9 kg	47%	185 kg	349 kg	809 kg	869 kg	2.0 kg	4.5%

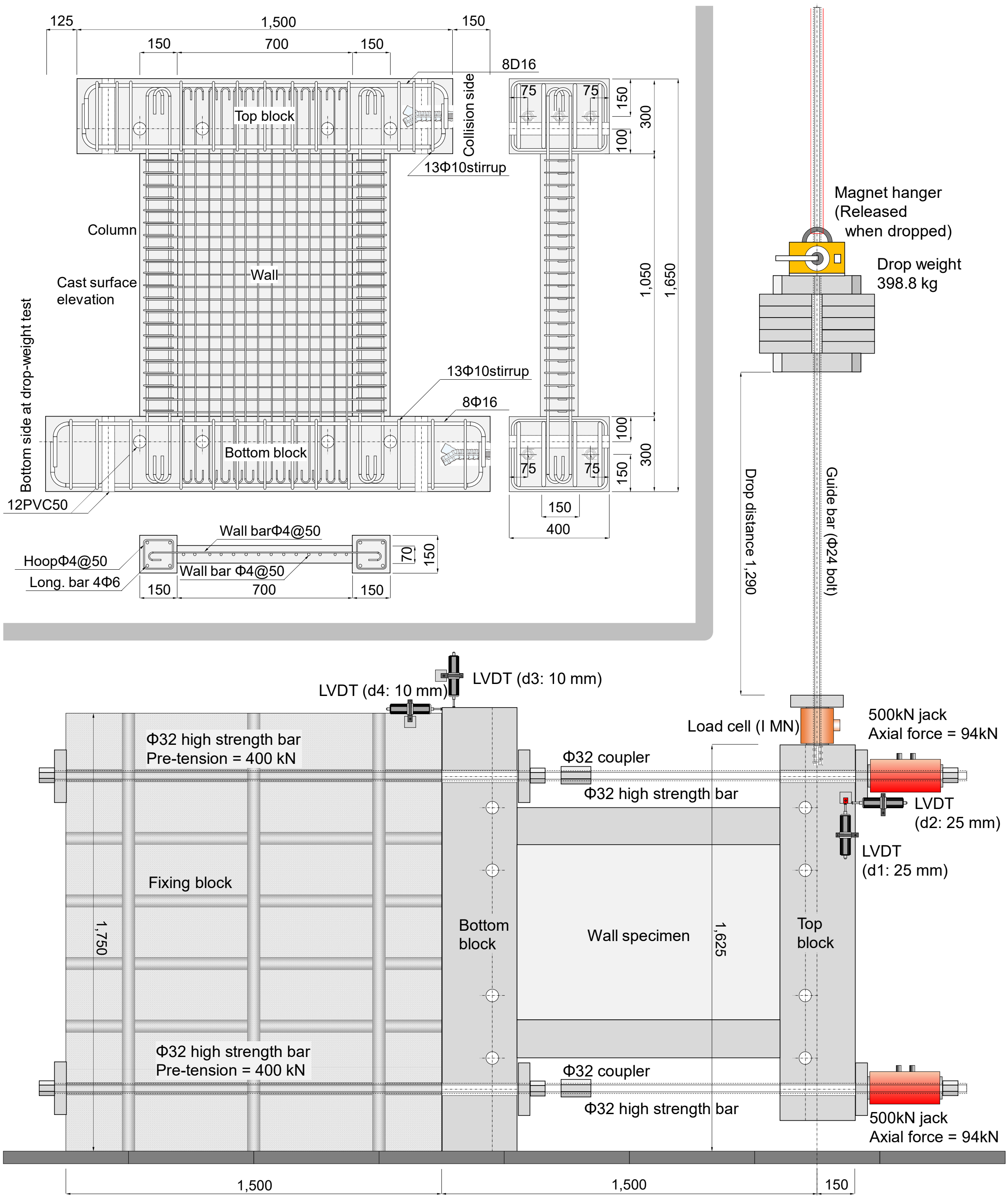

Fig. 1 – Wall specimen and test instrumentations (unit: mm)

2.2 Drying condition and strength development

The wall specimens are subjected to two kinds of drying shrinkage conditions. Specimens N0 and P0 are subjected to 21-day drying without any restraint. Figure 2 shows relationship between the shrinkage strain and the material day and Fig. 3 the temperature and the relative humidity of the corresponding period. The shrinkage strain before the drop-weight test is 1.344×10^{-3} for the plain concrete of N0 and 0.993×10^{-3} for the PFRC of P0, respectively. The average temperature during this period is 24.2°C and the average relative humidity 71.0%. Figure 4 shows developments of the compressive strength, the elastic modulus, the strain corresponding to the compressive strength, and the tensile strength. Each value attains more than 90% of the 28-day property within seven material days.

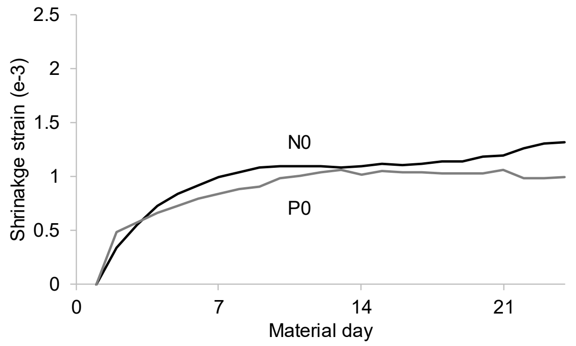

Fig. 2 – Relationship between drying shrinkage strain and material day of concrete for N0 and P0

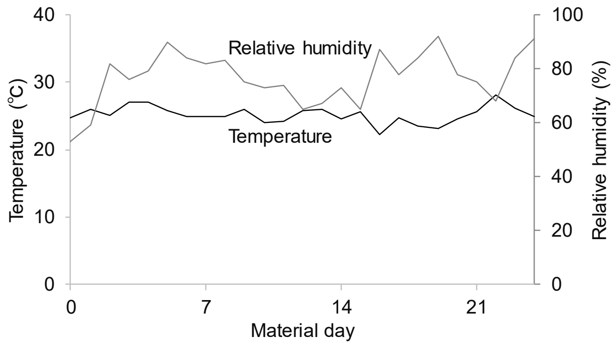

Fig. 3 – Relationship between temperature, relative humidity and material day of concrete for N0 and P0

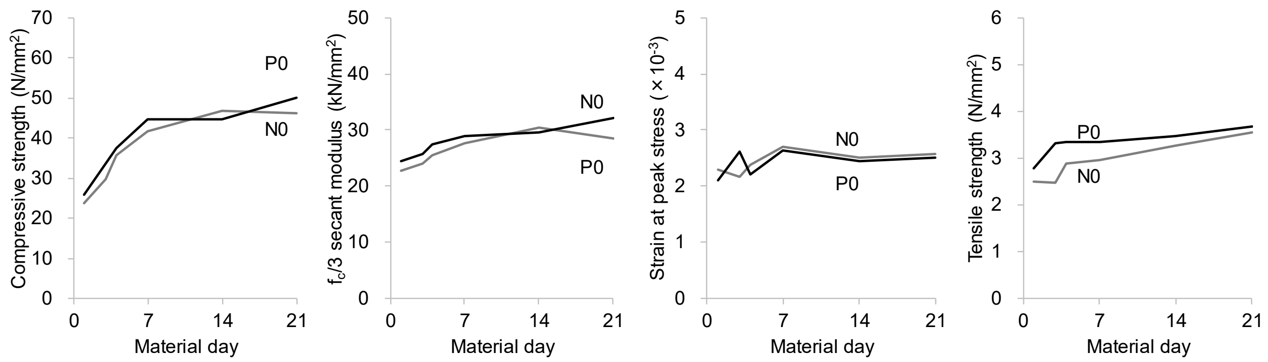

Fig. 4 – Developments of compressive strength, elastic modulus, strain corresponding to compressive strength, and tensile strength of concrete for N0 and P0

On the other hand, NR and PR are subjected to one-year drying with restraining. After the casting and removing the formwork, the top and bottom blocks are fixed to a strong steel reaction wall by eight high strength bolts by applying each 179 kN tension to restrain the shrinkage deformation of the wall as shown in Fig. 5(a). Specimens for the free shrinkage tests are made into blocks of size 100 × 100 ×500 mm. Two free shrinkage specimens are prepared for each wall specimen. Figures 6, 7 and 8 show the shrinkage strains, the temperature, the relative humidity, and the developments of material properties. The shrinkage strain before the drop-weight test is 1.877×10^{-3} for the plain concrete of NR and 1.031×10^{-3} for the PFRC of PR, respectively. The average temperature during this period is 17.0°C and the average relative humidity 65.2%. The shrinkage strain of the PFRC is equivalent to that of 21-day and almost half of the plain concrete.

(a) Restraining of NR on strong steel reaction wall

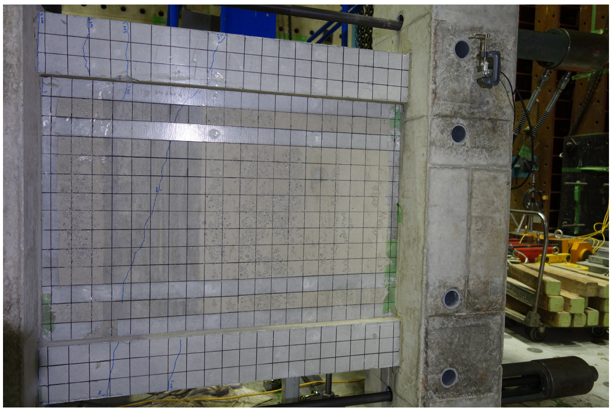

(b) Condition of NR after drop-weight test

(c) Drop-weight test instrumentations

Fig. 5 – Photographs of tests

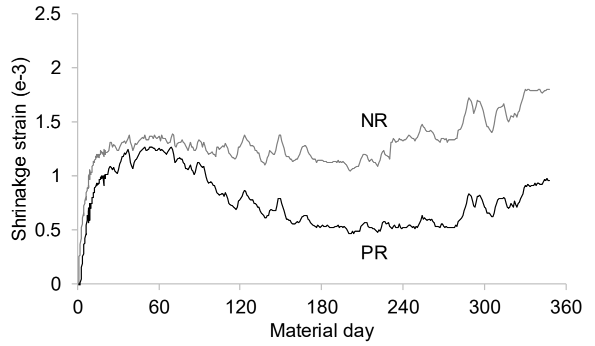

Fig. 6 – Relationship between drying shrinkage strain and material day of concrete for NR and PR

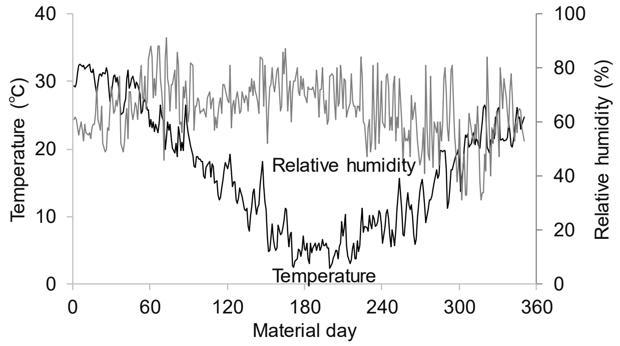

Fig. 7 – Relationship between temperature, relative humidity and material day of concrete for NR and PR

Figure 9 shows the relationships between compressive stress and strain of the concretes obtained by cylinders of 100 mm diameter and 200 mm height. Numbers in the legends denote the material day. The PFRCs of Specimens P0 and PR present higher stresses in the post-peak stage comparing to those of the plain concretes although the pre-peak behaviors are almost identical.

Figure 10 shows the relationships between load and crack opening displacement of three-point bending specimens of 100 × 100 mm cross section and 400 mm clear span with a central groove of 20 mm depth. The volume ratio of the polypropylene fiber content is varied by 0%, 0.6%, 1.2% and 1.8% although only two of the four are used for the wall specimens. As expected, the residual load becomes larger as the volume ratio becomes larger. Figure 11 shows the back-analyzed tension softening characteristics of the plain concrete for N0 and NR (0%) and the PFRC for P0 and PR (1.2%). The residual stress of the latter is 0.67 N/mm^2, which is maintained until the fiber length is completely pulled-out from the concrete matrix. This characteristics will be used for the finite element analyses in the following section.

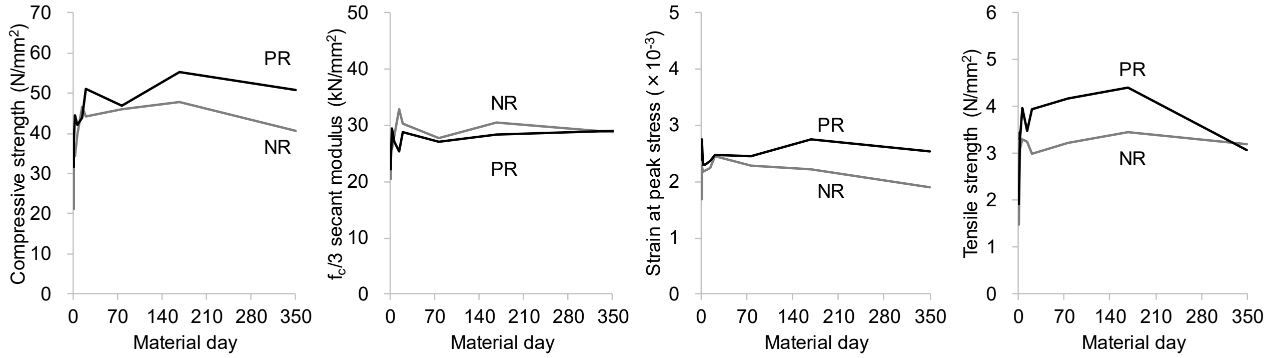

Fig. 8 – Developments of compressive strength, elastic modulus, strain corresponding to compressive strength, and tensile strength of concrete for NR and PR

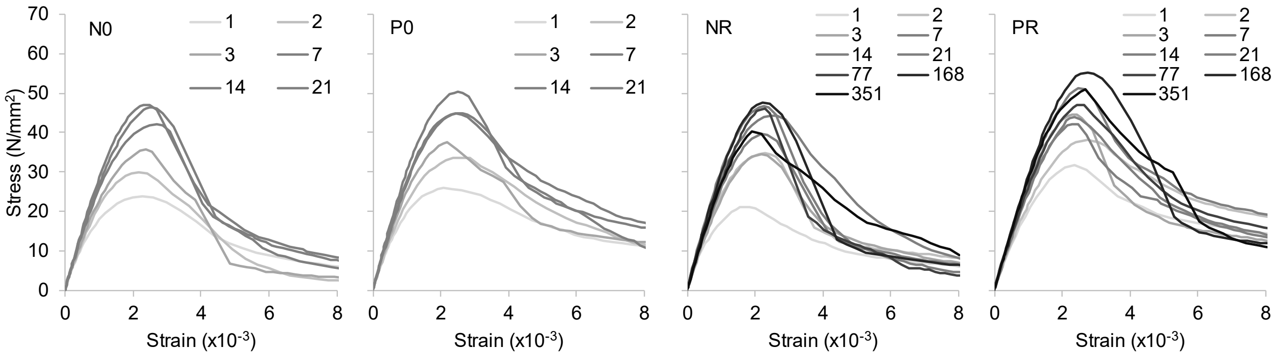

Fig. 9 – Relationships between compressive stress and strain of concretes

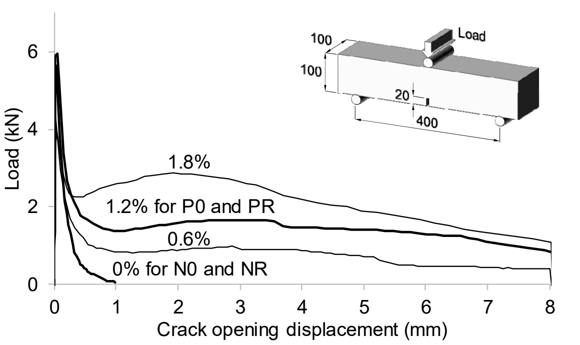

Fig. 10 – Relationship between load and crack opening displacement of three-point bending tests

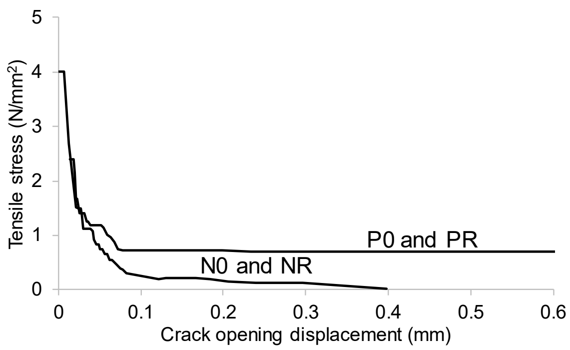

Fig. 11 – Back-analyzed tension softening characteristics

2.3 Drop-weight tests

The drop-weight tests are conducted by the instrumentation shown in Fig. 1 and Fig. 5(c). Each specimen is rotated 90° and fixed to a concrete block. Axial forces of total 188 kN are applied by two externally aligned high-strength bars tensioned by two hydraulic jacks on the top block. A drop weight composed of steel plates is hung by a magnet hanger and released from a height of 1.29 m. A constant velocity of 5 m/s is applied at the instance of collision. The masses of the drop weight is 398.8 kg. According to the impact tests of beam specimens by Saatci [6], the ratio of the energy absorbed by a specimen to the kinetic energy of the drop weight ranges from 6% to 32%, and the ratio depends on the shear reinforcement ratio and the kinetic energy of the drop weight. In this study, the masses of the drop weight is determined based on the assumptions that (1) the ratio of energies is assumed as 15%; (2) the expected ultimate drift of the wall specimen is 0.5%; and (3) the drop height is constant. A load cell of 1000 kN capacity is inserted between the specimen and the drop weight. Four displacement transducers are fixed on the specimen to measure the horizontal and vertical displacements of the top block (d1 and d2) and the slip and separation of the bottom block (d3 and d4). The drift is defined by Eq. (1):

$$\text{Drift} = (\text{d1(mm)} - \text{d3(mm)} - \text{d4(mm)} \times 1500\ \text{mm} / 1775\ \text{mm}) / 1050\ \text{mm} \tag{1}$$

Equation (1) indicates that the drift is calculated form the top drift (d1) by subtracting the slip (d3) and the rotation (d4 ×height / width). The sampling frequency is 5 kHz and the duration is 0.3 second.

Table 1 summarizes the test results. Figures 12 and 13 show time histories of the drifts and loads, respectively. The maximum drifts are: N0 0.649%, NR 0.637%, P0 0.635%, and PR 0.687%. The residual drifts, defined as average drifts during the time from 0.1 to 0.3 second, are: N0 0.057%, NR 0.150%, P0 -0.015%, and PR 0.102%. The maximum loads are: N0 717.2 kN, NR 775.5 kN, P0 780.1 kN, and PR 764.3 kN. The maximum drifts and loads of the four walls are almost equivalent while the residual drift of NR is noticeably large comparing to those of the rest three walls.

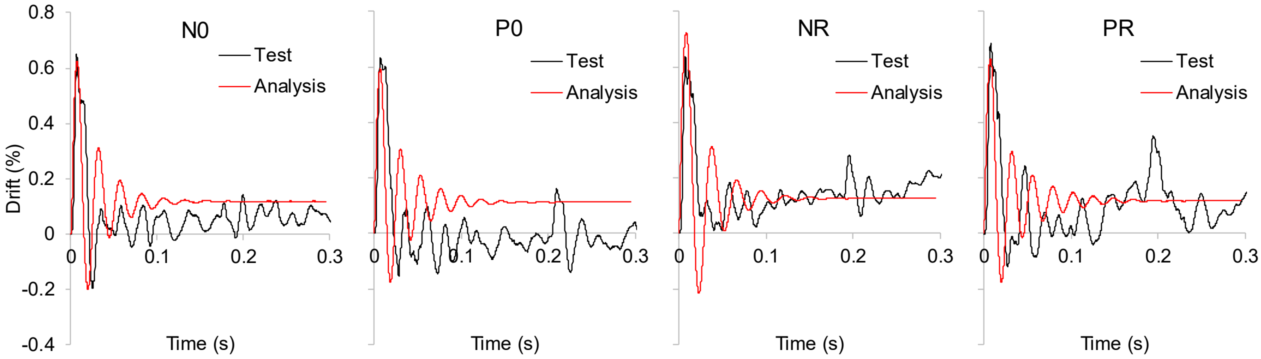

Fig. 12 – Relationships between drift and time

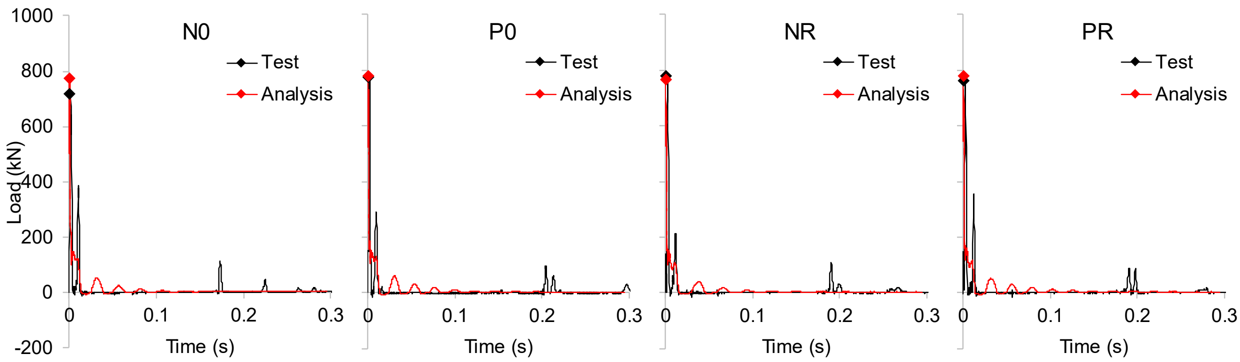

Fig. 13 – Relationships between load and time

Figure 14 shows the crack patterns. Before the drop-weight tests, cracks of 0.05 mm widths are found only in NR. After the test, a flexural crack along the boundary between the wall and the bottom block is observed in all the specimens. The crack widths of NR is widened up to 0.10 mm although the existing cracks are not extended. No concrete crushing nor bar rupturing are observed as shown in Fig. 5(b).

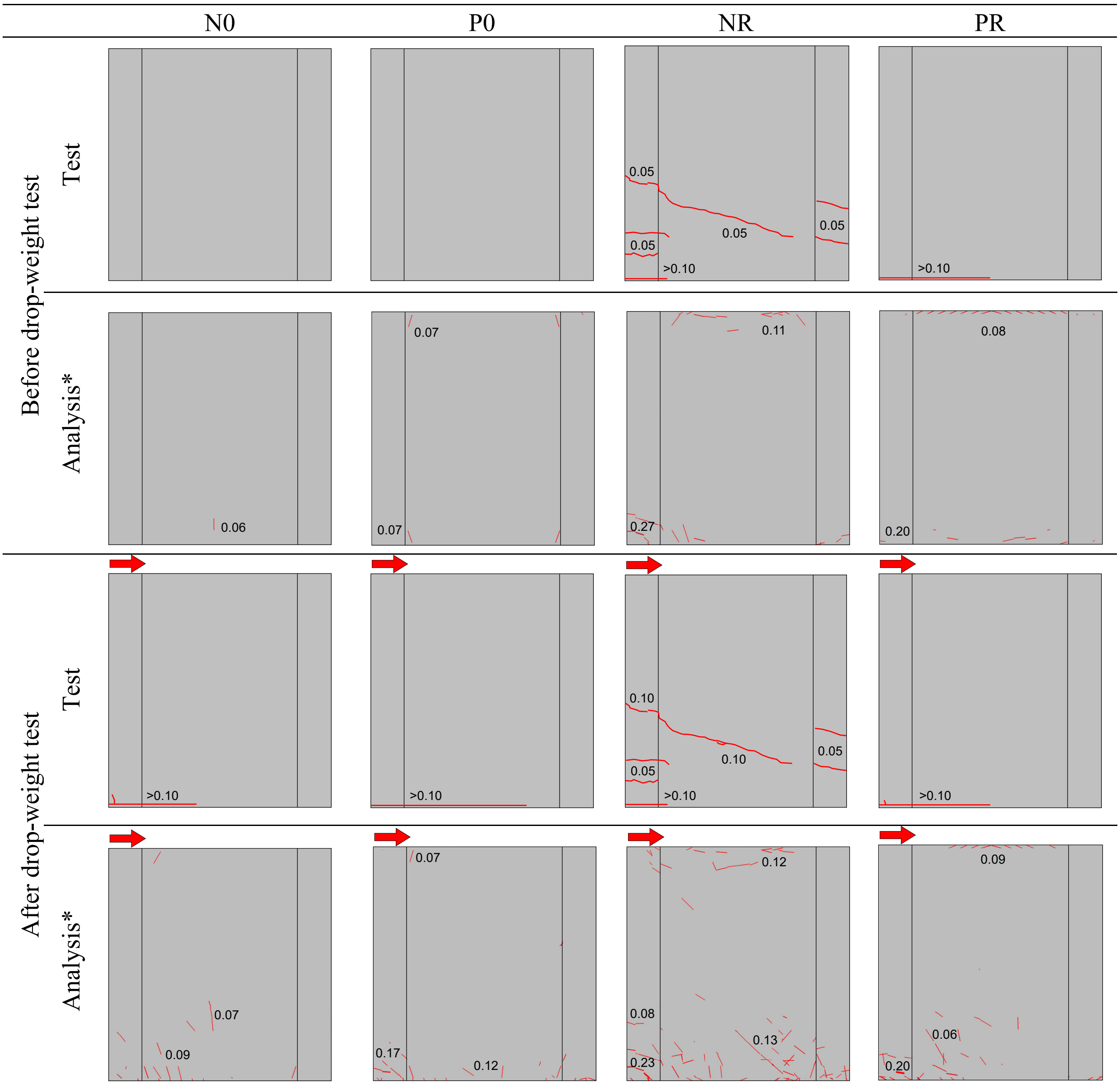

Fig. 14 – Crack patterns before and after drop-weight test (*cracks smaller than 0.05 mm width are erased.)

3. Analyses

A 2D mesh shown in Fig. 15(a) is prepared to numerically reproduce the walls' behaviors. A nonlinear FEM program that can analyze the response history over time is used [7, 8, 9]. The concrete part, the load cell, and the drop weight are modeled by four-node quadrilateral elements (total 866 elements) and the longitudinal steel bars in the columns and the external high-strength bars are modeled by two-node truss elements (total

136 elements). The shear reinforcements are modeled by embedded smeared reinforcement in the quadrilateral concrete elements. The static cyclic response of this model had already been examined as mentioned above [4] (Fig. 15(b)). Forty-six two-node joint elements are inserted between the bottom block and the fixing boundary to provide the rigid reaction under compression and the free separation under tension. Six two-node joint elements are inserted between the top block, the load cell, and the drop weight to model strain-rate-dependent contacts. All the elements are defined by linear interpolation function so that analytical stability in the nonlinear state is enhanced. The total degrees of freedom of the model are 1892.

Figures 15(c), 15(d), 15(e), and 15(f) show the constitutive models of concrete [7] for the compression side, the tension side, the compression-tension transfer paths, and the shear transfer paths, respectively. The strain rate dependencies of the compressive and tensile strengths of concrete are considered based on Fujikake's research [10], and the yield stress of steel based on Hosoya's research [11], as shown in Fig. 15(g). The polypropylene fiber reinforcement effects are modeled as the tension softening characteristics after cracking, shown in Fig. 11. The analyses in this paper adopt the smeared crack model associated with fixed crack formulation, so the shear transfer model along the cracked surface is applied. For concrete crack propagation, the discretization method of crack distribution is applied [8, 9]. For the stress-strain relationship of steel in a bar, the Ciampi's model involving the Bauschinger effect is used (Fig. 15(h)) [12]. The shrinkage cracking is analyzed prior to the drop-weight dynamic analyses. Sixty percent of the shrinkage strains shown in Figs. 2 and 6 are input to each specimen by the material age increment of 0.05 day up to seven days and 0.175 day up to a year. The input strains are reduced because the shrinkage strain is partially released by tensile creep [13, 14].

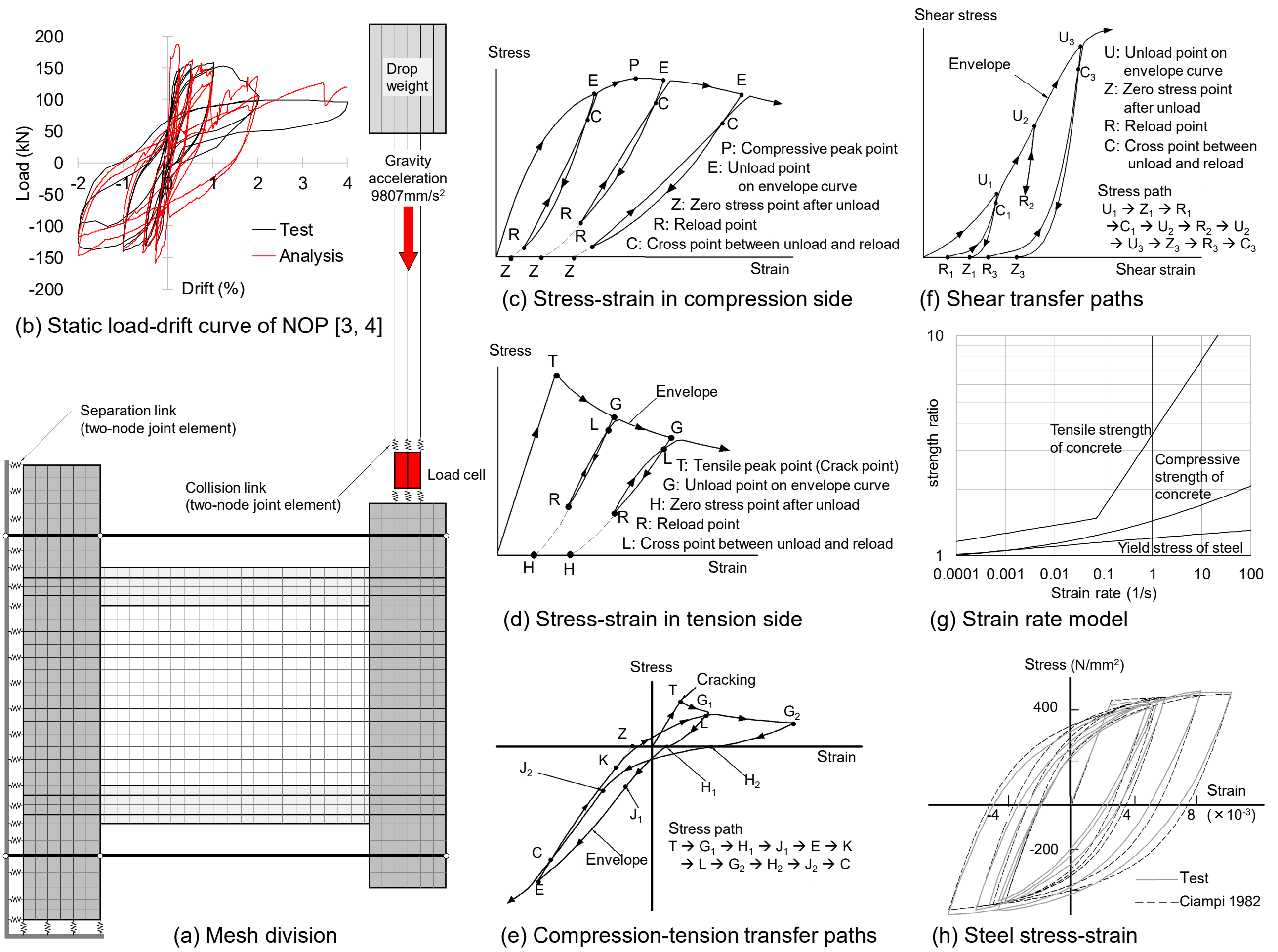

Fig. 15 – Mesh division and constitutive models

The dynamic analyses are conducted by applying the gravity acceleration of 9807 mm/s^2 to the entire model. Stiffness of the two-node joint elements between the top block, the load cell and the drop weight is determined by adopting a stiffness equivalent to either smaller stiffness of the materials in the two sides. For example, the joint element between the concrete top block and the steel load cell always adopts the former. The joint element stiffness is renewed step by step depending on the stiffness of crushed concrete. The time increment is 0.0001 second. The Newmark-β time integration method is adopted with parameters β = 0.25 and γ = 0.5 with uniform 1% damping proportional to the initial stiffness assumed for the first natural period of 0.00856 second, which is evaluated by eigenvalue analysis using the subspace method. Figures 12, 13 and 14 compare the time histories of drift and load and the crack patterns between the tests and the analyses. Cracks smaller than 0.05 mm width are erased from Fig. 14 since they are invisible to human eyes. The analyses well simulate the overall behaviors as well as the significant cracking in Specimen NR.

4. Discussion

Figure 16 compares the load-drift curves between the tests and the analyses, demonstrating the analyses' accuracy. The load attains the peak at the drift around 0.03% and descends rapidly. This behavior considerably differs to the relatively ductile response observed in the static loading shown in Fig. 15(b). The load begins to descend when the contact between the drop weight and the top block is released but the kinetic energy of the former has already been transferred to the latter, so the wall continues to drift by the inertia with the load descending.

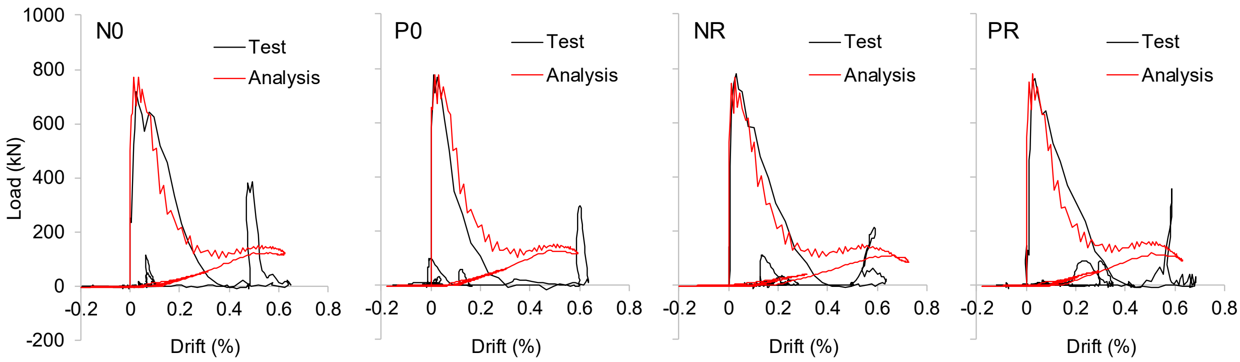

Fig. 16 – Relationships between load and drift

Figure 17 compares propagations of the drifts and the cracks between NR and PR from the maximum load step up to the maximum drift step. Typical shear/flexural deformations are observed in the both walls but the polypropylene fiber obviously reduces the amount of cracks of PR comparing to that of NR.

Figure 18 shows spectrums derived from the drift-time relationships shown in Fig. 12. The spectrums exclude the initial collision part at the time from 0.0 to 0.075 second because this part contains relatively large plastic deformation and are classified into three parts from 0.075 to 0.150 second, from 0.150 to 0.225 second, and 0.225 to 0.300 second, respectively. The peak amplitude is found at the period between 0.01 to 0.03 second in each specimen. Figure 19 shows the time histories of first, second and third mode natural periods of the walls evaluated by the subspace eigenvalue analyses considering the degraded stiffness of the plasticized concretes and steels. The first mode natural period ranges from 0.021 to 0.028 second, which matches with the peaks of spectrums in Fig. 18. The deformation mode also agrees with those shown in Fig. 17, so the first mode can be regarded as the dominant mode of this problem. The first mode natural period of NR is initially 0.024 second and elongated up to 0.028 after the collision, which is considerably larger than those of the rest three. This observation implies that the RC wall is weakened during the long period shrinkage and probably excites the seismic vibration of the building. On the other hand, the first mode natural period of PR is almost constant around 0.022 second, indicating that the polypropylene fiber prevents the elongation of natural period even after one-year drying shrinkage under the restraining.

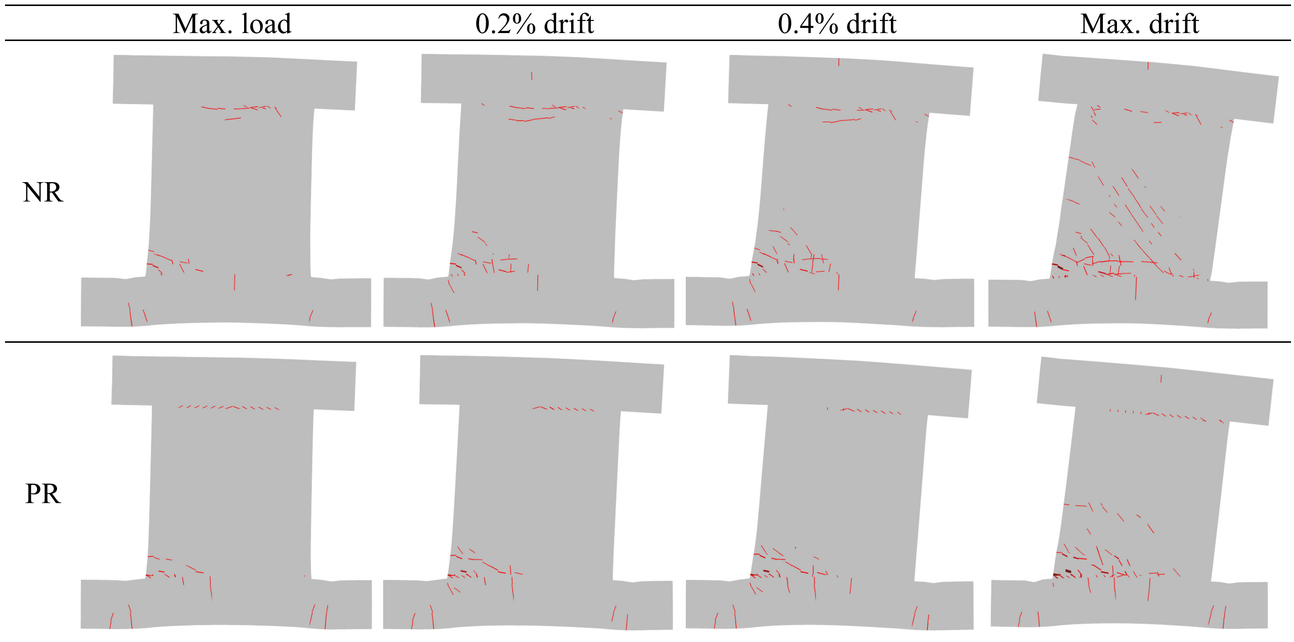

Fig. 17 – Propagations of drifts and cracks of NR and PR (cracks smaller than 0.05 mm width are erased.)

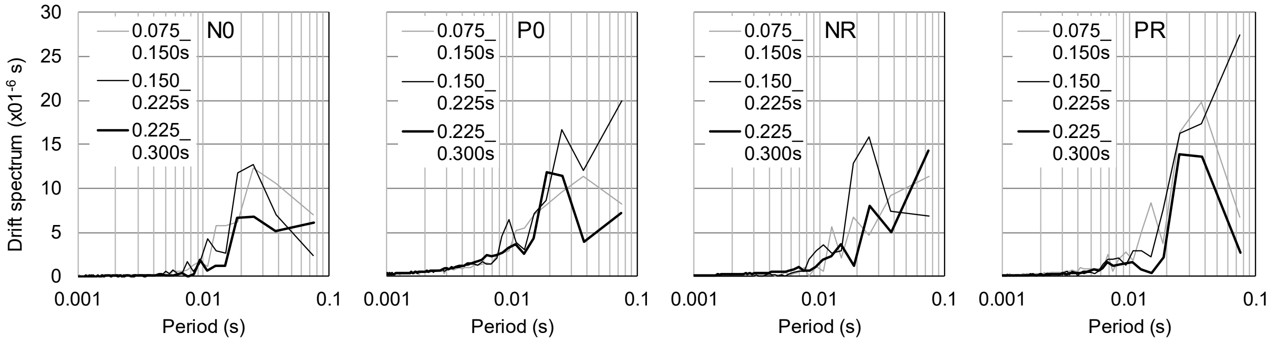

Fig. 18 – Drift spectrums derived from drop-weight test

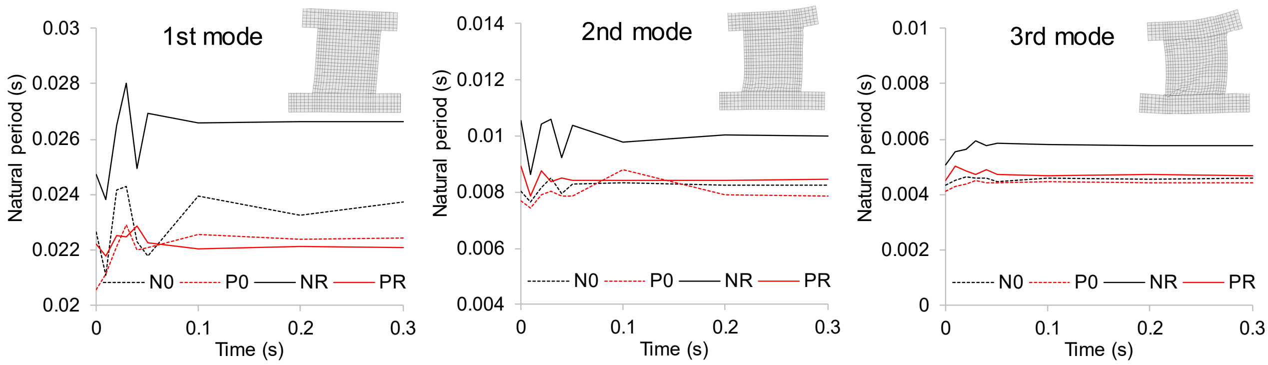

Fig. 19 – Time histories of first, second and third mode natural periods evaluated by eigenvalue analyses

5. Conclusions

The following remarks are made based on the drop-weight tests and the finite element analyses of the RC walls:

(1) One-year drying shrinkage under the restrained condition induces significant cracking to the RC wall made of the plain concrete.

(2) The PFRC reduces the cracks induced by the shrinkage under the same restraining condition.

(3) The PFRC also reduces the cracks induced by the drop-weight collision and prevents the elongation of the natural period.

This work is supported by MEXT / JSPS KAKENHI Grant-in-Aid for Scientific Research (C), 18K04430.

6. References

[1] Kurihara R, Chijiwa N and Maekawa K (2017): Thermo-Hygral Analysis on Long-Term Natural Frequency of RC Buildings with Different Dimensions. *Advanced Concrete Technology*, **15**, 381-396, DOI: 10.3151/jact.15.381.

[2] Kitazawa K, Sato Y, Naganuma K and Kaneko Y (2018): Finite Element Analyses of Seismic Response of a 22-story RC Wall Building subjected to Drying Shrinkage Cracking and Application of SCRPCC. *Proceedings of Fibre Reinforced Concrete: from Design to Structural Applications (FRC 2018), ACI-fib-RILEM Joint Workshop*, 104-109.

[3] Iwamoto H and Tsuda K (2016): An experimental study on flexural behavior of reinforced concrete shear walls with openings. *Proceedings of the Japan Concrete Institute*, **38(2)**, 679-684 (in Japanese).

[4] Akai F, Tajima K, Naganuma K and Sato Y (2017): Plastic strain energy based damage indices for concrete structures. *Journal of Structural Engineering*, Architectural Institute of Japan, **82(742)**, 1925-1933 (in Japanese).

[5] Makita K, Uda, Y, Yoshikado H, Mori K, Sato Y, Naganuma K and, Kaneko Y (2018): Drop-Weight Test For RC Frame Made of Polypropylene Fiber-Reinforced Concrete. *Advanced Concrete Technology*, **16**, 36-45.

[6] Saatci S and Vecchio FJ (2009): Nonlinear Finite Element Modeling of Reinforced Concrete Structures under Impact Loads. *ACI Structural Journal*, **106(5)**, 717-725.

[7] Naganuma K, Yonezawa K, Kurimoto O and Eto H (2004): Simulation of nonlinear dynamic response of reinforced concrete scaled model using three-dimensional finite element method. *Proceedings of the 13th World Conference on Earthquake Engineering*, 586.

[8] Sato Y and Naganuma K (2007): Discrete-like crack simulation by smeared crack-based FEM for reinforced concrete. *Journal for Earthquake Engineering and Structural Dynamics*, **36**, 2137-2152, DOI: 10.1002/eqe.720.

[9] Sato Y and Naganuma K (2014): Discrete-like crack simulation of reinforced concrete incorporated with analytical solution of cyclic bond model. *ASCE Journal of Structural Engineering*, **140(3)**, 109-116, DOI: 10.1061/(ASCE)ST.1943-541X.0000864.

[10] Fujikake K, Senga T, Ueda N, Ohno T and Katagiri M (2006): Study on impact response of reactive powder concrete beam and its analytical model. *Advanced Concrete Technology*, **4(1)**, 99-108.

[11] Hosoya H, Okada T, Kitagawa Y, Nakano Y and Kumazawa F (1996) Fiber Model Analysis of Reinforced Concrete Members with Consideration of the Strain Rate Effect. *Journal of Structural and Construction Engineering*, Architectural Institute of Japan, **482**, 83-92 (in Japanese).

[12] Ciampi V, Eligehausen R, Bertero V V and Popov E P (1982): Analytical model for concrete anchorages of reinforcing bars under generalized excitations. Report No. UCB/EERC-82/23, Univ. of California, Berkeley.

[13] Hong S, Sato Y, Kaneko Y and Kimura S (2015): Prediction of Drying Shrinkage Cracking of Eco-efficient Steel Chip Reinforced Cementitious Composite Considering Tensile Creep, *Advanced Concrete Technology*, *13*, 393-402, DOI: 10.3151/jact.13.393.

[14] Ida Y, Hong S, Kimura S, Sato Y and Kaneko Y (2016): Prediction of Drying Shrinkage Cracks of Steel Chip Reinforced Polymer Cement Mortar, *Advanced Concrete Technology*, **14**, 739-752, DOI: 10.3151/jact.14.739.

